

# Anomalous Kondo effect of indirectly coupled double quantum dots

Qing-feng Sun<sup>1,2</sup>, Hong Guo<sup>2</sup>, and Yupeng Wang<sup>1</sup>

<sup>1</sup>*Institute of Physics, Chinese Academy of Sciences, Beijing 100080, China*

<sup>2</sup>*Center for the Physics of Materials and Department of Physics, McGill University, Montreal, PQ, Canada H3A 2T8*

We report theoretical investigations of indirectly coupled double quantum dots (QD) side connected to an one-dimensional quantum wire. Due to quantum interference controlled by the parameter  $k_FL$ , with  $k_F$  the Fermi wave number of the wire and  $L$  the distance between the two QDs, distinctly different Kondo resonances are predicted depending on the range of  $k_FL$ . A true bound Kondo states is found while an anomalous Kondo resonance gives rise to both reduction and enhancement of conductance.

72.15Qm, 73.23Ad, 73.21.-b

In the original Kondo physics concerning magnetic impurities in metal<sup>1</sup>, effects of multiple impurities have been subjected to extensive study dating back to the 1960's<sup>2</sup>. Impurity scattering is characterized by a parameter  $k_F l_m$  where  $k_F$  is the Fermi wavevector of the host metal and  $l_m$  is the mean momentum relaxation length<sup>2</sup>. Impurities in a metal are situated randomly and typically one studies an *average* physical behavior. The recent extensive investigations of Kondo phenomenon in quantum dot (QD) devices, both theoretically and experimentally<sup>3,4</sup>, is due partly to the fact that such an important and prototypical many-body physics can be systematically investigated using QDs whose parameters are precisely controllable. However, despite the numerous investigations of QD Kondo effect, to the best of our knowledge, the QD parameter playing a similar role as the  $k_F l_m$  of a metal, has not yet been explored.

In this paper we report a theoretical investigation of Kondo effect in a device where two QDs side-couple to the same quantum wire but otherwise no direct coupling of any sort between them, as shown in Fig.(1a). Of particular interest is the dimensionless device parameter  $k_FL$  where  $k_F$  is the Fermi wavevector of the quantum wire and  $L$  the distance between the two QD's. Clearly,  $k_FL$  plays the role of  $k_F l_m$  of a metal, except that it can be precisely controlled to give unambiguous results about strongly correlated effects in quantum transport at reduced dimensions. There are several theoretical studies of Kondo physics in two QDs connected in series<sup>5,6</sup>, but systems studied so far all involve direct QD-QD coupling either through a tunnel coupling between the QD's or/and through the QD-QD Coulomb interaction. Experimentally, double-QD Kondo physics also starts to attract attention<sup>7</sup>. The present work will focus on the role of  $k_FL$ .

For a single QD weakly coupled to two leads in the form of Lead-QD-Lead, the signature of Kondo effect is

the *enhancement* of device conductance<sup>8</sup> as temperature  $T$  is lowered to below the Kondo temperature  $T_K$ . On the other hand, for a single QD side-coupled to a quantum wire, the signature of Kondo effect is the *reduction* of conductance of the quantum wire<sup>9</sup>. The QD Kondo effect is due to quantum superposition of electron cotunneling events<sup>1</sup> which is illustrated by the energy diagram shown in Fig.(1b) for a side-coupled single QD, where two electrons with different spins tunnel in/out of the QD in very short time scales. Below  $T_K$ , the Kondo effect makes the QD an efficient scatterer for electrons traversing the quantum wire thereby reducing conductance while screening spin of the QD.

For the device we consider (Fig.(1a)), although there is no direct QD-QD coupling, an electron may still flow from a QD to the other through the quantum wire, *i.e.* there is an *indirect* coupling between the QDs controlled by the parameter  $k_FL$ . Due to multiple reflections between the two QDs, quantum interference effect is found to give rise to a qualitatively different Kondo behavior in this device as compared to that of a single side-coupled QD system<sup>9</sup>. In particular, we found that a most general behavior for this system is that physical quantities such as local density of states (LDOS), transmission coefficient  $T(E)$ , and conductance  $G$ , are all periodic functions of parameter  $k_FL$  with a period of  $\pi$ . The Kondo effect is now separated into two distinct regimes given by  $k_FL < \pi/2$  and  $k_FL > \pi/2$ . For  $0 < k_FL < \pi/2$ , Kondo resonance can both reduce or enhance conductance of the quantum wire—qualitatively different from a single QD device.<sup>8,9</sup> On the other hand for  $\pi/2 < k_FL < \pi$ , Kondo effect can only reduce conductance. Exactly at  $k_FL = \pi$ , a true bound Kondo state is established in the region of the two QDs such that transport along the wire is drastically diminished by many orders of magnitudes.

The system of Fig.(1a) can be described by the Anderson Hamiltonian (not shown). For simplicity we consider a single level  $\epsilon_j$  ( $j = 1, 2$  labels the QD) in each QD with spin index  $\sigma$  ( $N = 2$  fold degenerate), and a constant on-site Coulomb interaction  $U$ . In the  $U \rightarrow \infty$  limit, double occupancy of  $\epsilon_j$  becomes unlikely therefore the on-site interaction does not occur, hence one can neglect  $U$  but enforcing the single occupancy of  $\epsilon_j$ . This idea is realized in the slave-boson approach<sup>5,10</sup> which we will use, and our results are qualitatively reasonable in the large  $U$  limit. In the slave-boson representation<sup>5,10</sup>, the Hamiltonian of the Anderson model describing the device is then transformed to the following form:<sup>5,11</sup>

$$H = \sum_{k\sigma} \epsilon_k c_{k\sigma}^\dagger c_{k\sigma} + \sum_{\sigma j} \frac{t_j}{\sqrt{N}} \left[ c_\sigma^\dagger (a_j) b_j^\dagger f_{j\sigma} + H.c. \right]$$

$$+ \sum_{\sigma j} \epsilon_j f_{j\sigma}^\dagger f_{j\sigma} + \sum_j \lambda_j \left[ b_j^\dagger b_j + \sum_{\sigma} f_{j\sigma}^\dagger f_{j\sigma} - 1 \right] \quad (1)$$

where  $c_{k\sigma}^\dagger (c_{k\sigma})$  is the electron creation (annihilation) operator in the one-dimension quantum wire with corresponding energy  $\epsilon_k = \frac{\hbar^2 k^2}{2m} + U_0$ , here  $m$  is the effective mass of the electron and  $U_0$  the potential energy in the quantum wire.  $b_j$  and  $f_{j\sigma}$  are the slave-boson operator and the pseudofermion operator, respectively. The last term represents the single-occupancy constraint  $b_j^\dagger b_j + \sum_{\sigma} f_{j\sigma}^\dagger f_{j\sigma} = 1$  in each QD with Lagrange multiplier  $\lambda_j$ . The two QDs are side-coupled to the quantum wire at positions  $x = a_j$  ( $j = 1, 2$ ), with  $t_j$  the tunneling matrix element. Finally, the annihilation operator  $c_\sigma(x)$  at position  $x$  is given by  $c_\sigma(x) = \int \frac{dk}{\sqrt{2\pi}} c_{k\sigma} e^{ikx}$ . In the following, we adopt a mean field theory in which the slave-boson operator  $b_j$  is taken as a constant c-number which is solved self-consistently. The mean field theory has been known to give a qualitatively good description of Kondo physics at low temperatures with zero bias voltage.<sup>5,11</sup>

To obtain conductance  $G$  and intradot LDOS, we calculate the retarded Green's functions  $G^r$  for Hamiltonian (1) from their definitions,  $G^r(xt, x'0) \equiv -i\theta(t) < \{c_\sigma(xt), c_\sigma^\dagger(x'0)\} >$  and  $G_{ij}^r(t, 0) \equiv -i\theta(t) < \{f_i(t), f_j^\dagger(0)\} >$ , where continuous variables  $x, x'$  are for the quantum wire and discrete indices  $i, j$  for the two QDs. If the QDs and the quantum wire do not couple ( $t_1 = t_2 = 0$ ), these Green's functions can be solved exactly and we denote them by  $g^r(x, x', E)$  and  $g_{ij}^r(E)$ :<sup>12</sup>  $g^r(x, x', E) = -i\pi\rho(E)e^{ik|x-x'|}$ ,  $g_{ij}^r(E) = \delta_{ij}/(E - \tilde{\epsilon}_j + i0^+)$ , where all time dependence have been Fourier transformed into energy  $E$  dependence. Here  $k = \sqrt{2m(E - U_0)/\hbar}$ ,  $\tilde{\epsilon}_j = \epsilon_j + \lambda_j$ , and LDOS of the wire is  $\rho(E) = \frac{m}{\pi\hbar^2 k}$ . Using  $g^r(x, x', E)$ ,  $g_{ij}^r(E)$  as unperturbed Green's function and apply Dyson equation with terms involving  $t_j$  as the potential, we obtain exactly

$$G^r(x, x', E) = g^r(x, x') + \sum_{i,j} g^r(x, a_i) \tilde{t}_i G_{ij}^r \tilde{t}_j g^r(a_j, x') \quad (2)$$

$$G_{jj}^r(E) = \frac{g_{jj}^{r-1} - \Sigma_j^r}{(g_{jj}^{r-1} - \Sigma_j^r)(g_{jj}^{r-1} - \Sigma_j^r) - \Sigma_j^r \Sigma_j^r e^{2ikL}}$$

$$G_{j\bar{j}}^r(E) = \tilde{t}_j g^r(a_j, a_{\bar{j}}) \tilde{t}_{\bar{j}} G_{j\bar{j}}^r / (g_{j\bar{j}}^{r-1} - \Sigma_{j\bar{j}}^r)$$

where  $\bar{j} = 2$  if  $j = 1$ , or  $\bar{j} = 1$  if  $j = 2$ ;  $\tilde{t}_j = \frac{t_j b_j}{\sqrt{N}}$ ; and  $L = |a_1 - a_2|$ . The self-energy  $\Sigma_j^r(E) = \tilde{t}_j^2 g^r(a_j, a_j, E) \equiv -\frac{i}{N} \Gamma_j(E) b_j^2 \equiv -i\tilde{\Gamma}_j$ . From  $G^r$ , the transmission coefficient  $T(E)$ , conductance  $G$ , and intradot LDOS $_j(E)$  can all be calculated<sup>12</sup> straightforwardly:  $T(E) = |i\hbar v G^r(a_1, a_2, E)|^2$ ,  $G = \frac{2e^2}{h} \int dE T(E) \left( \frac{-\partial f(E)}{\partial E} \right)$ , and LDOS $_j(E) = -\frac{1}{\pi} \text{Im} G_{jj}^r(E)$ . Here  $v = \frac{\hbar k}{m} = 1/\pi\hbar\rho(E)$  is the electron velocity and  $f(E)$  the Fermi distribution of the quantum wire. Finally, the above analysis is supplemented with a self-consistent numerical calculation of the four unknowns  $b_j$  and  $\lambda_j$ . From the

constraints and the equation of motion of the slave-boson operators,<sup>5</sup> we derive the self-consistent equation as:  $b_j^2 + \sum_{\sigma} n_{j\sigma} = 1$  with the intradot electron occupation number  $n_{j\sigma} = \int dE f(E) \text{LDOS}_j(E)$  and  $\lambda_j b_j^2 = \sum_{\sigma} \int \frac{dE}{\pi} f(E) \text{Im} [g_{jj}^r(E) \tilde{t}_j^2 G^r(a_j, a_j, E)]$ .

In the following, we fix the chemical potential  $\mu$  of the quantum wire as the energy zero, and assuming that  $U_0$  has a large negative value,  $-U_0 \gg \max(k_B T, \Gamma_j, |\epsilon_j|)$ , so that the wave vector  $k$  and the density of state  $\rho(E)$  can be approximated as independent of  $E$  at  $E \sim \mu$ . This way  $\Gamma_j(E)$  is also approximately a constant and  $k \approx k_F$ . We consider square symmetric bands in which  $\Gamma_j(E) = \Gamma_j \theta(W - |E|)$  and  $W = 100 \gg \max(k_B T, \Gamma_j, |\epsilon_j|)$ . Finally, we set  $\Gamma_1 = \Gamma_2 \equiv \Gamma = 1$  as the energy unit. We now discuss results.

**LDOS and bound Kondo states.** Due to multiple reflections between the two QDs, LDOS,  $T(E)$  and  $G$  are all periodic functions of parameter  $k_F L$  with a period  $\pi$ . If each QD acts independently, then each has its own Kondo resonance at energy  $\tilde{\epsilon}_0$  with a width  $\tilde{\Gamma}_0 = \frac{\Gamma b^2}{N}$  and Kondo temperature  $k_B T_K^0 = \sqrt{\tilde{\epsilon}_0^2 + \tilde{\Gamma}_0^2} = W e^{-\pi|\epsilon_0|/\Gamma}$ . With coherence, however, there is a superposition of these individual Kondo states through multiple scattering between the two QDs. For example, if the two QDs are identical ( $\epsilon_1 = \epsilon_2 \equiv \epsilon$  and  $\tilde{\epsilon}_1 = \tilde{\epsilon}_2 \equiv \tilde{\epsilon}$ ), coherent superposition establishes two new Kondo peaks: peak-1, at energy  $(\tilde{\epsilon} + \frac{\tilde{\Gamma}}{2} \sin k_F L)$  with half-width  $\frac{\tilde{\Gamma}}{2}(1 + \cos k_F L)$ ; and peak-2, at energy  $(\tilde{\epsilon} - \frac{\tilde{\Gamma}}{2} \sin k_F L)$  with half-width  $\frac{\tilde{\Gamma}}{2}(1 - \cos k_F L)$ .<sup>13</sup> The thin solid curve (red) in Fig.(1c) plots the LDOS of this situation at  $k_F L = \pi/2$  for which the two Kondo peak heights are almost equal, while other values of  $k_F L$  (dotted and dashed curves) make unequal peak heights.

A very interesting situation is when  $k_F L = n\pi$  where  $n$  is an integer: the width of one of the Kondo resonances vanishes because of the factor  $(1 \pm \cos k_F L)$ . This means a true bound Kondo state is localized in the region of the two QDs within energy continuum. The thick solid curve (blue) in Fig.(1c) plots the LDOS of the device with  $k_F L = 0.99\pi$ , showing a very sharp Kondo peak with tiny width. This peak evolves into a  $\delta$ -function exactly at  $k_F L = \pi$ . Fig.(1a) shows the physics behind the bound Kondo state. During the frequent co-tunneling processes which gives rise to Kondo effect, an electron can tunnel out of QD-1 and flow away in the quantum wire, indicated by path-1 (p1) of Fig.(1a). But this electron can also flow towards QD-2 to participate co-tunneling there and afterward it flows back, as shown by path-2 (p2). If  $k_F L = n\pi$ , path-1 and path-2 will differ by a phase difference of  $(n\pi + \pi + n\pi) = (2n + 1)\pi$ , resulting to a destructive interference. It is the quantum superposition of these destructive interferences which prevents the electron from flowing away from the two QD region, and therefore a bound Kondo state. It is very interesting to observe that electrons participating Kondo resonance

can be completely bounded, and this has important effect to the conductance of the quantum wire (see below).

The above behavior qualitatively holds when the two QDs are not totally identical. However, as the difference  $\Delta\epsilon \equiv \epsilon_1 - \epsilon_2$  becomes large, the two QDs act more independently and the two Kondo peaks gradually localize themselves into the QDs. With a small but finite  $\Delta\epsilon$  and with  $k_FL = \pi$ , the bound Kondo state (peak-1, see above) develops a tiny width, much smaller than  $k_BT_K^0$ , but it now further coherently superposes with the other Kondo state (peak-2) to produce a Fano-like interference line shape, as shown in Fig.(1d).

**Transmission coefficient.** Quantum interference also gives rise to an anomalous behavior in  $T(E)$ . For a single side-coupled QD,  $T(E)$  should simply decrease when  $E$  is near the Kondo resonance  $\tilde{\epsilon}_0$ , and reach its minimum  $T = 0$  for energy  $E = \tilde{\epsilon}_0$  due to Kondo scattering. For our two QD device, this is still largely true as shown in Fig.(2) where  $T(E) \sim 1$  when  $E$  is far away from  $\tilde{\epsilon}$  and  $T(E)$  takes small values when  $E \sim \tilde{\epsilon}$ . However, due to multiple scattering between the two QDs during the co-tunneling processes, a resonance transmission become possible similar to the optical interference of a Fabry-Perot interferometer. This induces a very sharp peak  $T(E) = 1$  near  $E \approx 0$  in the otherwise small  $T(E)$  background, see Fig.(2). This resonance peak exists regardless of the value of  $k_FL$ , but importantly the peak position  $E^*$  crucially depends on whether or not  $k_FL > \pi/2$ , as we found  $E^* = \tilde{\epsilon} - \frac{\tilde{\Gamma}}{2} \frac{\sin k_FL}{\cos k_FL}$ . Hence, if  $\pi/2 < k_FL < \pi$ ,  $E^*$  is always positive (i.e.  $E^* > \mu$ ) for any intradot level  $\epsilon$  (see Fig.2b), so that this  $T(E^*)$  peak does not contribute to conductance at Fermi level. On the other hand, for  $0 < k_FL < \pi/2$ ,  $E^*$  can become zero (i.e.  $E^* = \mu$ ) or negative which depend on the intradot level  $\epsilon$  as shown by the inset of Fig.(2), and the resonance  $T(E^*)$  peak can therefore contribute to Kondo effect. Due to this  $T(E^*)$  peak which originates from quantum interference, conductance  $G$  will also show an anomalous behavior as we show now.

**Conductance.** For identical QDs, Fig.(3a) plots  $G$  versus the intradot level  $\epsilon = \epsilon_1 = \epsilon_2$  at finite but low temperature  $\mathcal{T}$  with different values of  $k_FL$ . For both high ( $\epsilon > \mu = 0$ ) and very low  $\epsilon$ ,  $G$  is quite large,  $G \sim 2e^2/h$ . This is because transport is not in the Kondo regime and  $G$  is given by the one channel ballistic wire. On the other hand, when  $\epsilon \sim -2\Gamma$  the device is in the Kondo regime, and  $G$  is strongly affected by scattering of the two side-coupled QDs. For  $\frac{\pi}{2} < k_FL < \pi$ , the scattering causes  $G$  to strongly reduce when  $\epsilon \sim -2\Gamma$ . Although there is still a peak in  $T(E^*)$  at  $E^* > 0$  for this range of  $k_FL$ , this peak plays no role to Kondo effect as we discussed in the last paragraph. Hence, qualitatively, the Kondo effect for  $\frac{\pi}{2} < k_FL < \pi$  is similar to that of a single side-coupled QD device.<sup>9</sup>

The behavior of  $G$  becomes qualitatively different for  $0 < k_FL < \frac{\pi}{2}$ , because the anomalous  $T(E^*)$  peak will now contribute to Kondo physics. The striking conse-

quence is that  $G$  can now both decrease and increase in the Kondo regime, the latter is due precisely to the anomalous  $T(E^*)$  peak. Hence, as shown in Fig.(3a),  $G$  has two asymmetric dips and one peak in the region  $\epsilon \sim -2\Gamma$ . Letting temperature  $\mathcal{T}$  decrease, the dip becomes deeper and the peak becomes higher with a slight change of their positions toward lower  $\epsilon$ . The anomalous Kondo effect also shows up in temperature dependence of  $G$  for  $0 < k_FL < \frac{\pi}{2}$ . As shown in Fig.(3b) where  $k_FL = \frac{\pi}{6}$ ,  $G$  becomes non-monotonic as  $\mathcal{T}$ :  $G \sim 2e^2/h$  for high  $\mathcal{T}$  ( $\mathcal{T} > T_K^0$ ), it decreases as  $\mathcal{T}$  decreases and becomes lower than  $T_K^0$ , but it increases again and even can reach  $2e^2/h$  at much lower  $\mathcal{T}$ . The increase of  $G$  is surprising since the device is in the Kondo regime and incident electrons should be back-scattered strongly by the two side-coupled QDs. This increase of  $G$  is due to the  $T(E^*)$  peak at  $E^* \sim 0$  discussed above. In other words, quantum interference due to multiple reflections by the two QDs enhances the conductance of the wire in the Kondo regime, an anomalous behavior indeed.

Finally, when  $\frac{\pi}{2} < k_FL < \pi$ , since the  $T(E^*)$  peak does not contribute to the Kondo effect,  $G$  is simply a monotonic decreasing function of temperature in the Kondo regime, shown in Fig.(3c) and (3d). For instance, with  $k_FL = \frac{\pi}{2}$ ,  $G \sim 2e^2/h$  at high  $\mathcal{T}$  ( $\mathcal{T} > T_K^0$ );  $G$  then decreases substantially and eventually saturates at  $\sim 10^{-2}e^2/h$  at low  $\mathcal{T}$  due to Kondo scattering. An interesting situation is when  $k_FL \rightarrow \pi$  for which the true bound Kondo state is established as discussed above. This causes  $G$  to reduce much more to values less than  $10^{-9}e^2/h$  for  $k_FL = 0.99\pi$ . In fact, as  $k_FL \rightarrow \pi$ ,  $G \rightarrow 0$ .

In summary, we found that the dimensionless parameter  $k_FL$  provides a critical control of the Kondo phenomenon in the double-QD device where the QDs side-couple to a quantum wire but otherwise no direct coupling between them. Due to interference of quantum paths of electrons participating the co-tunneling process, a new Kondo behavior is predicted. In particular, a true bound Kondo state, an anomalous resonance peak in transmission coefficient, as well as anomalous conductance behavior, are found depending on the range of  $k_FL$ . The predicted phenomena should be experimentally observable using present technologies. The two side-coupled QD's device can be fabricated in two-dimensional electron gas (2DEG). Using Fermi wave length  $\lambda_F \sim 50\text{nm}$  for typical 2DEG,  $L \sim 25\text{nm}$  gives  $k_FL = \pi$  while  $L \sim 38\text{nm}$  gives  $k_FL = \frac{3\pi}{2}$ , hence the interesting Kondo effect of this device controlled by parameter  $k_FL$  can be accessed experimentally.

**Acknowledgments:** We gratefully acknowledge financial support from NSERC of Canada, FCAR of Quebec (Q.S., H.G), the National Science Foundation of China and the Chinese Academy of Sciences (Q.S. and Y.W).

- <sup>1</sup> J. Kondo, Prog. Theor. Phys. (Kyoto) **32**, 37 (1964). For a recent review, see for example, L. Kouwenhoven and L. Glazman, Physics World, (January, 2001), p33.
- <sup>2</sup> R.H. Bresemann and M. Baily, Phys. Rev. **154**, 471 (1967); M.T. Beal-Monod, Phys. Rev. **178**, 874 (1969); B.A. Jones and C.M. Varma, Phys. Rev. Lett. **58**, 843 (1987); P. Schlottmann, *ibid.* **80**, 4975 (1998).
- <sup>3</sup> T. Inoshita, Science **281**, 526 (1998); S. M. Cronenwett, *et al*, Science **281**, 540 (1998); D. Goldhaber-Gordon, *et al*, Nature **391**, 156 (1998); Phys. Rev. Lett. **81**, 5225 (1998).
- <sup>4</sup> W. G. van der Wiel, *et al*, Science **289**, 2105 (2000); S. Sasaki, *et al*, Nature **405**, 764 (2000).
- <sup>5</sup> R. Aguado and D.C. Langreth, Phys. Rev. Lett. **85**, 1946 (2000).
- <sup>6</sup> A. Georges and Y. Meir, Phys. Rev. Lett. **82**, 3508 (1999); L. Borda, *et al*, *ibid.* **90**, 026602 (2003); R. Lopez, R. Aguado, and G. Platero, *ibid.* **89**, 136802 (2002). R. Aguado and D.C. Langreth, Phys. Rev. B **67**, 245307 (2003); Q.-f. Sun and H. Guo, *ibid.* **66**, 155308 (2002).
- <sup>7</sup> H. Jeong, A.M. Chang, and M.R. Melloch, Science **293**, 2221 (2001).
- <sup>8</sup> Y. Meir, N.S. Wingreen, and P.A. Lee, Phys. Rev. Lett. **70**, 2601 (1993).
- <sup>9</sup> K. Kang, S.Y. Cho, J.-J. Kim, and S.-C. Shin, Phys. Rev. B **63**, 113304 (2001); T.-S. Kim and S. Hershfield *ibid.* **63**, 245326 (2001); A.A. Aligia and C.R. Proetto, *ibid.* **65**, 165305 (2002).
- <sup>10</sup> P. Cdeman, Phys. Rev. B **29**, 3035 (1984).
- <sup>11</sup> H. Hu, G.-M. Zhang, and L. Yu, Phys. Rev. Lett. **86**, 5558 (2001).
- <sup>12</sup> S. Datta, *Electronic Transport in Mesoscopic Systems* (Cambridge University, Cambridge, England 1995).
- <sup>13</sup>  $\tilde{\epsilon}$  is slightly different from  $\tilde{\epsilon}_0$  of a single QD. For  $U \rightarrow \infty$ ,  $\tilde{\epsilon}_0$  must be greater than zero (*i.e.*  $\mu$ ). But  $\tilde{\epsilon}$  may be a very small but negative number for some parameter values of  $k_F L$  and  $\epsilon$ .

FIG. 1. (a). Schematic diagram for the device where two QDs side-couple to a quantum wire. (b). Schematic diagram for a single side-coupled QD and its co-tunneling processes. (c). LDOS vs  $E$  for  $\epsilon_1 = \epsilon_2 = 2$  and  $k_F L = \frac{\pi}{3}$  (dotted curve),  $\frac{\pi}{2}$  (thin solid curve),  $\frac{2\pi}{3}$  (dashed curve), and  $0.99\pi$  (thick solid curve). (d). Left dot LDOS for  $k_F L = 0.99\pi$ ,  $\epsilon_{1/2} = 2 \pm \Delta\epsilon/2$ , and  $\Delta\epsilon = -0.05$  (dotted curve) and  $0.05$  (solid curve). Temperature  $\mathcal{T} = 0.02$  in (c) and (d).

FIG. 2.  $T(E)$  vs  $E$  for  $\mathcal{T} = 0.02$ . The parameters are:  $\epsilon = -1.6$  (dashed curve),  $-1.8$  (solid curve),  $-2.0$  (dotted curve), and  $-2.2$  (thin solid curve);  $k_F L = \frac{\pi}{6}$  (a) and  $\frac{5\pi}{6}$  (b). The inset amplifies the three curves of (a) near  $\mu = 0$ .

FIG. 3. (a): Conductance  $G$  vs  $\epsilon$  for  $\mathcal{T} = 0.01$  (dotted curve,  $k_F L = \frac{\pi}{6}$ ) or  $0.02$  (solid curve).  $k_F L$  of the solid curves along the arrow are for  $\frac{\pi}{6}$ ,  $\frac{\pi}{3}$ ,  $\frac{\pi}{2}$ ,  $\frac{2\pi}{3}$ , and  $0.99\pi$ , respectively. (b), (c), and (d):  $G$  vs  $\mathcal{T}$ . (b) is for  $k_F L = \frac{\pi}{6}$ , and along the arrow  $\epsilon = -1.6, -1.8, -2.0, -2.2$ , and  $-2.4$ , respectively. (d) plots  $G$  versus  $\mathcal{T}$ , and (c) is  $\log G - \log \mathcal{T}$ . The four thin curves are for  $k_F L = \frac{\pi}{2}$  and  $\epsilon = -1.7$  (dashed curve),  $-2.0$  (dot-dashed curve),  $-2.3$  (solid curve), and  $-2.5$  (dotted curve). The three thick curves are for  $\epsilon = -1.7$  and  $k_F L = 0.98\pi$  (dotted curve),  $0.988\pi$  (dashed curve), and  $0.99\pi$  (solid curve).

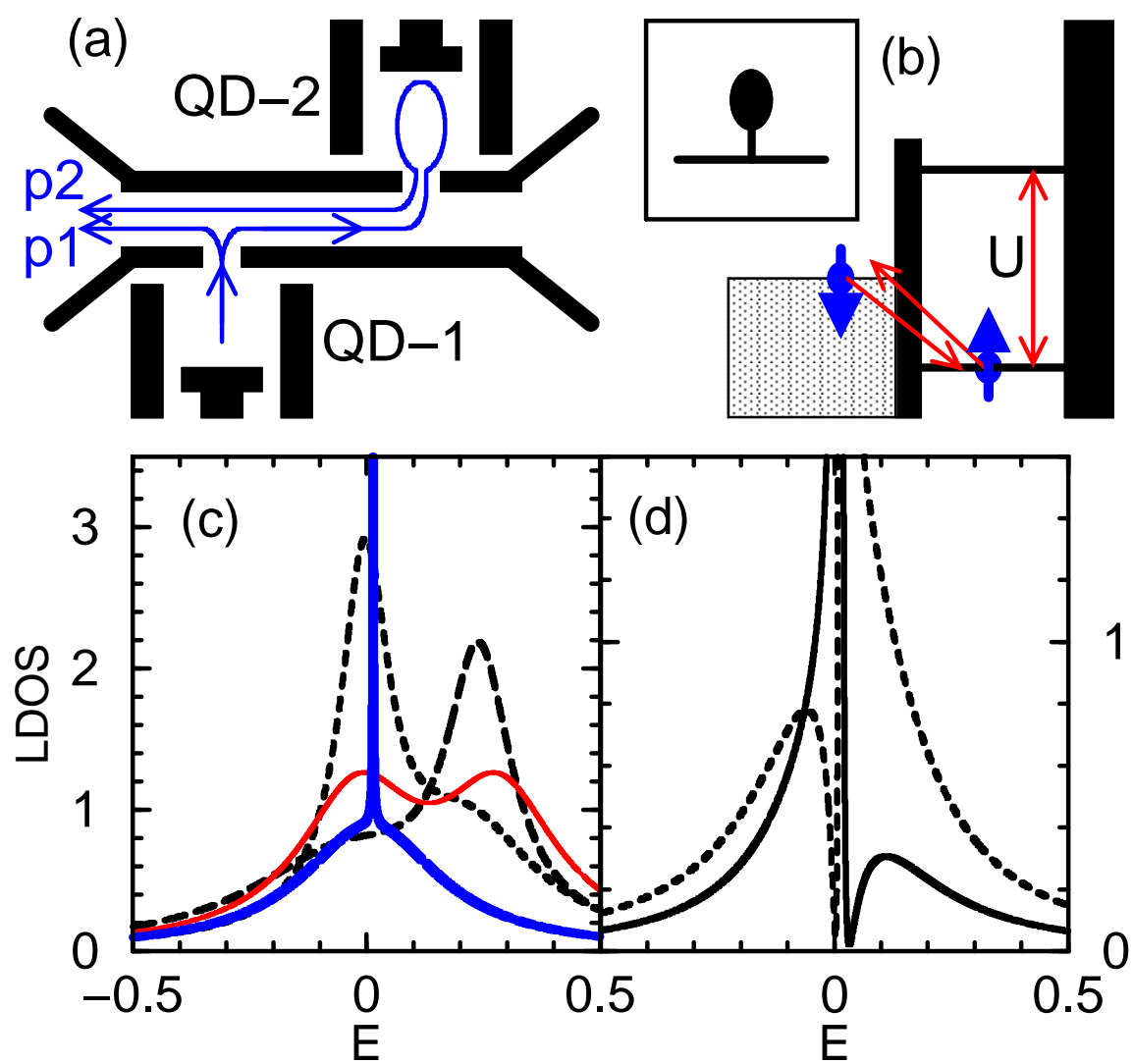


Fig.1

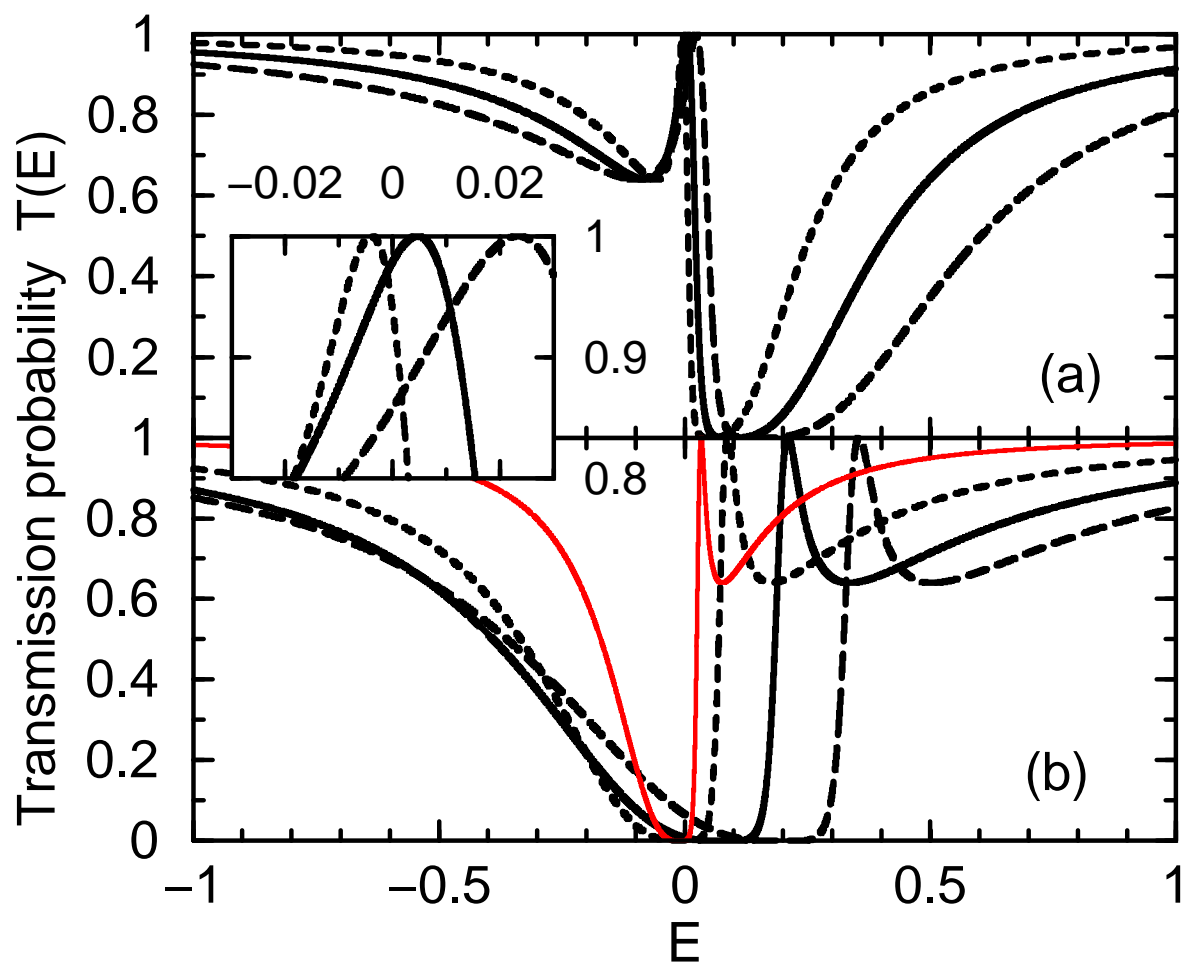


Fig.2

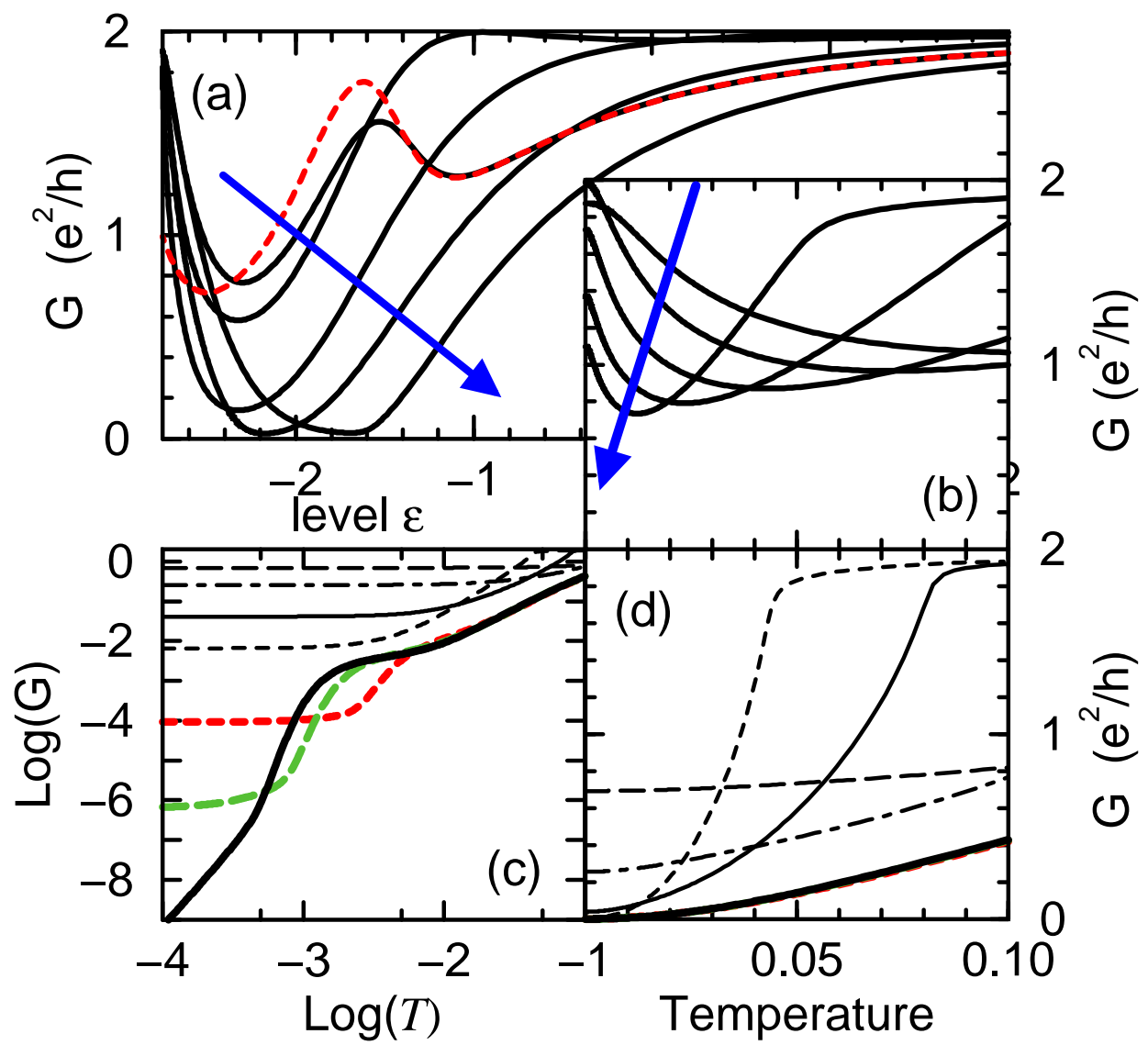


Fig.3